DETECTION OF H_α EMISSION ON HIGH VELOCITY 21 CM CLOUDS

Guido Münch and Eckhart Pitz
Max-Planck-Institut für Astronomie
Königstuhl, 6900 Heidelberg
FRG

ABSTRACT. The measurement of H_α emission on two high galactic latitude clouds known to emit 21 cm lines with local standard of rest (LSR) velocities of −50 and −85 km s^{-1} is reported. The H_α lines have been found nearly at the velocities of the 21 cm features and have emission rates of 0.2 Rayleigh. The diffuse Lyman continuum intensity required to produce HI ionization at the measured rate is in agreement with the direct measurements made with the ultraviolet (UV) spectrometer of the Voyager 2 spacecraft.

1. INTRODUCTION

Observations of interstellar absorption lines in a few stars at high latitude showed long ago (Münch, 1952; Münch and Zirin, 1961) the presence of interstellar gas at distances from the galactic plane $|z| \simeq 1$ kpc; this presence was unexpected because of the known distribution of interstellar clouds at the plane. The behavior of the CaII and NaI line components in the same stars also led us to suspect that the physical state (ionization) of that gas was different from that at the plane. The development of 21 cm astronomy, approximately contemporaneous with the optical observations, later provided a detailed and extensive view of the surface distribution and kinematics of the interstellar neutral gas at high latitude (Van Woerden et al., 1985, and references therein). Our knowledge of the height distribution and state of ionization of the gas at high z, however, has not been widened by radio astronomical studies. The presence of faint extended HII gas, essentially all over the sky, revealed by observations carried out with the wide-angle tandem Fabry-Perot spectrometer of the University of Wisconsin (Reynolds, Roesler, and Scherb, 1974, 1977; Reynolds, 1980, 1984) suggested to us a search for H_α emission in well-defined high-velocity clouds mapped in 21 cm. In this communication we present preliminary results to date obtained in the survey undertaken at the Calar Alto Observatory for this specific purpose.

2. OBSERVATIONAL PROCEDURES

The spectrometer we have built is basically identical to the Wisconsin Poly Etalon Pressure-Scanned Interferometric Optical Spectrometer (PEPSIOS). It consists of a 15 cm diameter objective Fabry Perot master etalon, piezoelectrically servo-controlled for plate parallelism and scannable over a range of 850 km s^{-1} at an order of interference m=2100 for H_α. An off-order suppressing etalon of 50 mm diameter has been coupled to the master with a gap ratio 1:8:12. The field stop, generally 0°.8 in diameter, is placed at an intermediate focus between etalons, while the interference prefilter (FWHM = 15 Å) stands in the parallel beam entering the slave etalon. We used Ga:As photomultiplier detectors for the scanned channel and for a

S. Bowyer and C. Leinert (eds.), The Galactic and Extragalactic Background Radiation, 193–198.

wide-band signal-monitoring sky transparency. The instrument has a vertical optical axis and is fed by a polar siderostat. The effective resolution at H_α has been measured to be 11 km s^{-1} (FWHM), the finesse of the entire system being 14. The large gap ratio between etalons leads to off-order ghosts of appreciable and objectionable intensity, spaced by 136 km s^{-1}. Disregarding prefilter transmission, the percentage intensities of m±n ghosts is 4.8, 1.9, 0.7, and 0.6, for n=1, 2, 3, and 4, with respect to the main tuned line.

Besides the geocoronal H_α, the strong OH airglow lines P_1 (3) 6553.66 and P_2 (4) 6568.78 of the (6,1) band produce ghosts only partially suppressed by the prefilter and slave etalon. The chosen spectral free range of the master etalon fortuitously has placed the ghosts of these two OH lines near those of H_α, thus providing relatively extended ranges free of known airglow features. The diverse variabilities in position and time of the airglow and geocoronal lines practically preclude the "subtraction" of the sky features from a given scan by a comparison with another scan taken on a neighboring field, necessarily not simultaneously. It should also be mentioned that the airglow line features appear superposed on a continuum of considerable intensity with unknown spectral characteristics and variable in time. Typically the continuum level of a scan obtained during a night of average photometric quality in Calar Alto, such as that in Figure 1, is measured to be around 15 cps (PM pulse counts per second), which after subtraction of photomultiplier (PM) dark current is approximately accounted for by unresolved direct starlight (2 cps), by zodiacal light (6 cps), and the rest by light scattered in the atmosphere from artificial illumination and background sources. The component due to zodiacal light and stars must have H_a in absorption, but it will have no effect except in distorting the geocoronal line slightly.

Daytime sky spectra taken with our spectrometer actually show H_α absorption with a relative depth of 40%, a consequence of its high level of parasitic light, but no other singly identifiable line. The continuously drawn curve over the sample points of Figure 1a is a best fit of two Gaussians to the main H_α line and its ghost. The spectrum obtained upon subtraction of the two Gaussians from the raw spectrum, shown in Figure 1b, illustrates the expected non-Gaussian form of the geocoronal line, besides sensible departures from a smooth continuum not resembling photon noise. The obvious mean slope of the apparent continuum is not seen in white light spectra, which only show a slight curvature at $v \leq -200$ and +40 km s^{-1}. The faint emission peaks at −230, −205, and −190 km s^{-1} are OH ghosts, but the rather pronounced absorptionlike feature at −155 km s^{-1} cannot be explained except as a vagary of sky transmission. Evidently, additional scans made exclusively to establish the shape of the true continuum would be necessary to decide on the reality of the two broad emissionlike features peaking around −135 and −100 km s^{-1}. In view of the uncertainties in the continuum such as that in Figure 1, shared by many of our scans, the important question to settle is the intensity level to which weak emission lines can be detected and measured with some degree of certainty.

Adopting as the photometric standard an emission rate of 850 R ($1R$=1 Rayleigh=2.47×10^{-7} erg cm^{-2} s^{-1} at H_α) for NGC7000, as determined by Scherb (1981) and independently confirmed by our measurements, we find that a line in Figure 1 with a peak signal equal to the mean dark count (2 cps) and instrumental width would correspond to an emission rate of 0.1 R. The measurement of narrow lines with emission rates no less than 0.2 R is thus entirely feasible even in single scans with 30 s integration time per sample. An emission rate of 0.2 R at H_α, from gas at 10^4 K corresponds to an emission measure EM=0.5 cm^{-6} pc. In this context it is of interest to recall that Hulsbosch (1975) believed that the minimum measurable EM "without losing radial velocity information" was 50, although at that time all the means to carry out measurements such as ours were available.

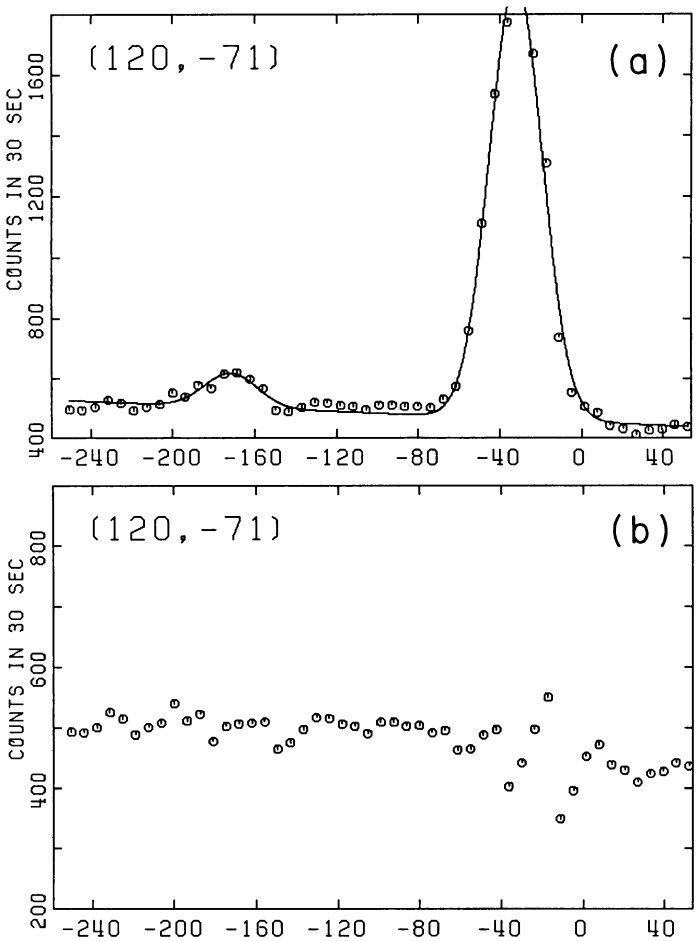

Figure 1. H_α spectrum of a region with galactic coordinates l=120°, b=–71°. (a) The coaddition of 4 scans, each with 30 s integrations per sample point, in a LSR velocity scale. The continuous curve is a Gaussian fit for the geocoronal H_α and its ghost. (b) The spectrum left after subtracting the fitted Gaussians for the geocoronal line and its ghost.

3. H_α EMISSIONS FROM TWO HIGH VELOCITY 21 CM CLOUDS NEAR THE NORTH GALACTIC POLE

The mean 21 cm profile toward the North Galactic Pole (NGP) (90° ≥ b ≥ 75°, 0° ≥ l ≥ 360°), obtained by Kulkarni and Fich (1985) from the Bell Telephone Laboratories HI Survey (Stark et al., 1989), is highly asymmetric in velocity, with more than 50% of all H_α falling toward the galactic plane with velocities up to −100 km s^{-1}. The actual surface and velocity distribution of high latitude HI shows a great deal of structural detail, ideally suited to search for velocity-shifted H_α that might be correlated in intensity with HI brightness temperature. The region of the OMM360 field of Meng and Krauss (1970), centered at RA = $10^h 18^m$ and

https://doi.org/10.1017/S0074180900240606 Published online by Cambridge University Press

DEC = +28°0, has been chosen because of the extent and brightness shown in the 21 cm maps (beam 10′) of Giovanelli, Verschuur, and Cram (1973) at –45 km s^{-1}. For comparison we have taken the feature OLM351, nearby in position and velocity to OMM360, which happens to cover completely the high velocity cloud OLH393 with V = –86kms^{-1}, also called MII by Hulsbosch (1968). The observations of an H_α component near –50 km s^{-1} on OMM360, together with the detection on OLH393 of H_α components near –50 and –80 km s^{-1}, would then provide strong evidence for a close relationship between the HI and HII emitting gases.

We have obtained scans at 10 positions in and around the OMM360 complex, all of which unmistakably show galactic H_α in the range –40 to –60 km s^{-1}. The average of two scans of the condensation at ($10^h 18^m$, 28°0) is shown in Figure 2a. The fit and subtraction of Gaussians for the geocorona and ghosts lead to the residual spectrum of Figure 2b, which

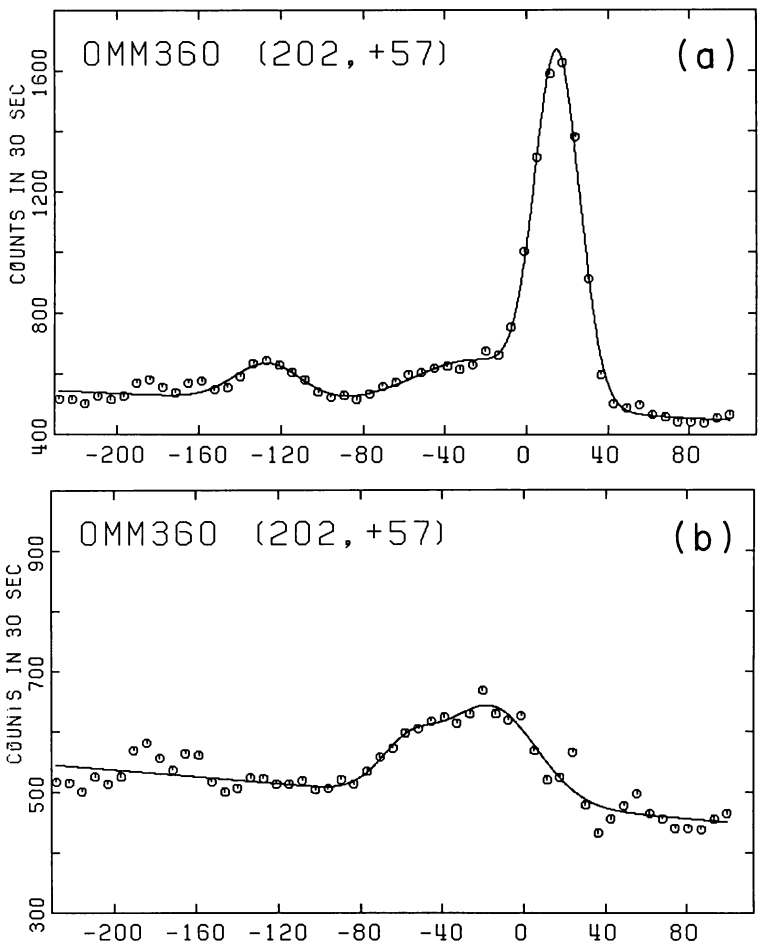

Figure 2. H_α spectrum of the 21 cm cloud OMM360 at l=202°, b=+57°. (a) The coaddition of two scans with a fit of three Gaussians for the geocoronal line, its ghost, and the galactic displaced emission. (b) The spectrum after subtraction of the fitted geocoronal line and ghost. The residual galactic emission has been fitted by two Gaussians.

https://doi.org/10.1017/S0074180900240606 Published online by Cambridge University Press

clearly shows a complex displaced H_α. The Gaussian fit of two components shown in Figure 2b has peaks at −54 and −14 km s^{-1}, half intensity width of 26 and 34 km s^{-1}, and emission rates of 0.35 and 0.85 R, respectively. Spectra obtained in fields outside the 21 cm boundaries of OMM360 and other nearby clouds also show the H_α component at −50 km s^{-1} somewhat weaker than within. Specifically, the west boundary of OMM360 in the map of Meng and Krauss (1970) appears at (10^h00^m, +30°0), but shifted galactic emission is noticeable in scans taken at 9^h20^m and the same declination.

Unlike OMM360, the OLH393 or MII cloud is relatively compact and small (4°×8°) (Giovanelli, Verschuur, and Cram, 1973), although it is probably a member of a "chain" of clouds extending to the northeast. A spectrum of OLH393, the result of the coaddition of two

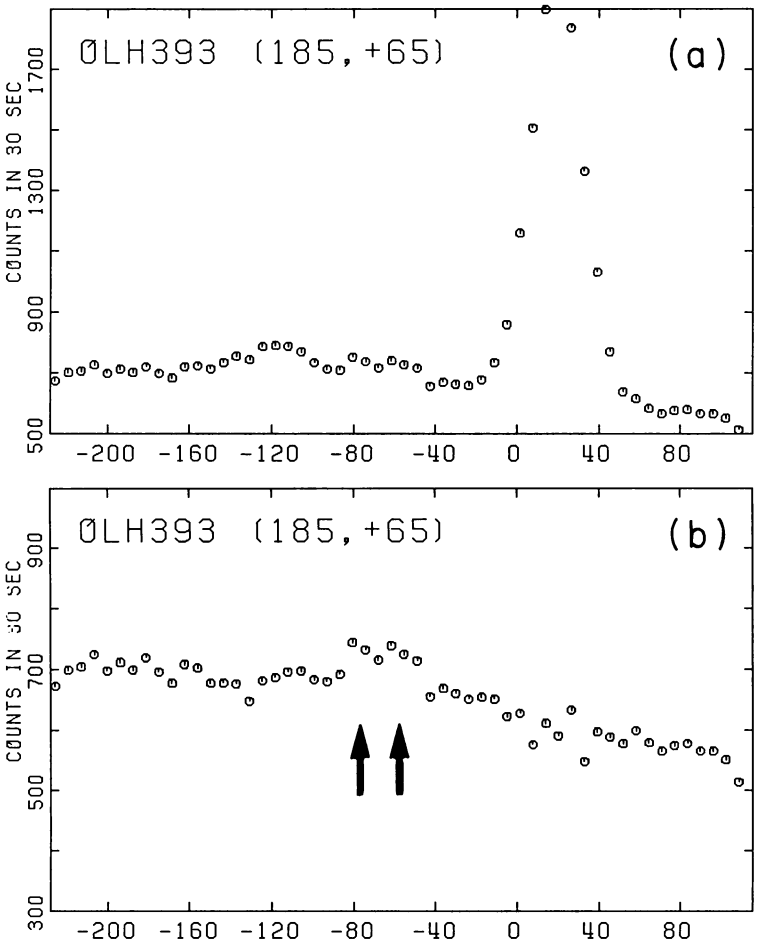

Figure 3. H_α spectrum of the 21 cm cloud OLH393 at l=185°, b=+65°. (a) The coaddition of two scans obtained on January 10 and 13, 1989. (b) The spectrum subtracted from the geocoronal line and ghost (fit not shown for clarity). The features highlighted with arrows are attributed to HII gas associated with OLH393 and OLH351.

https://doi.org/10.1017/S0074180900240606 Published online by Cambridge University Press

scans obtained in January 1989 at (11^h00^m, +36°.5) is shown in Figure 3a, which upon subtraction of Gaussian fits for the geocoronal H_α and its ghost leads to Figure 3b. The simple comparison of Figures 2a and 3a immediately shows the different shape of the spectra shortward of the geocoronal H_α and longward of its ghost, indicating less low velocity H_α in OLH393 than in OMM360 and the filling-in of the range immediately longward of the ghost. The reality of the two components in Figure 3b, with peaks near –80 and –50 km s^{-1}, is strongly suggested by the secondary minimum between the two components, appearing in six of the eight scans we have so far secured in the same field. In any case we can be certain that the displaced galactic emission in OLH393 extends beyond –80 km s^{-1}, unlike that in the spectrum of OMM360 in Figure 2b. On this basis we identify the –80 km s^{-1} feature as produced by HII gas associated with OLH393, while the accompanying –50 km s^{-1} line, at least in part, may be emitted by OLM351. The intensities of each of the two galactic displaced H_α lines in Figure 3b can be only approximately estimated to be in the range 0.1 to 0.2 R, because of uncertainties in fixing the line width and the continuum level in the scans available.

4. THE BACKGROUND UV RADIATION

The recent detection by Kutyrev and Reynolds (1989) of H_α in a very high velocity ($\approx$ –250 km s^{-1}) cloud together with our observations demonstrate the feasibility of studying the HII phase of the gas in the galactic halo. Fragmentary as such observations may appear, they imply the existence of a UV ionizing radiation of considerable intensity, as Reynolds (1984, 1987) has emphasized. Since H_α is emitted in 45% of all recombination processes (Pengelly, 1964; Case B, $T=10^4$ K), it follows that an emission rate of 0.2 R, such as that measured in OLH393, in equilibrium requires a diffuse Lyman continuum with mean intensity 7×10^4 ph cm^{-2} s^{-1} sr^{-1}. This value is consistent with the value 100–200 ph cm^{-2} s^{-1} sr^{-1} $Å^{-1}$ measured by Holberg (1986) with the UV spectrometer on the spacecraft Voyager 2 in the direction of the NGP, when integrated over the effective width (500 Å) of the Lyman continuum.

Acknowledgment—We express our thanks to R. J. Reynolds for communicating unpublished material to us and for friendly discussions.

REFERENCES

Giovanelli, R., Verschuur, G. L., and Cram, T. R. 1973, *Astr. Ap. Supp.*, **12**, 209.
Holberg, J. B. 1986, *Ap. J.*, **311**, 969.
Hulsbosch, A. N. M. 1968, *Studies of High Velocity Clouds*, Dissertation, Leiden Univ.
Hulsbosch, A. N. M. 1975, *Astr. Ap.*, **40**, 1.
Kulkarni, S. R., and Fich, M. 1985, *Ap. J.*, **289**, 792.
Kutyrev, A. S., and Reynolds, R. J. 1989, *Ap. J. Letters*, in press.
Meng, S. Y., and Krauss, S. D. 1970, *A. J.*, **75**, 535.
Münch, G. 1952, *P. A. S. P.*, **64**, 312.
Münch, G., and Zirin, G. 1961, *Ap. J.*, **133**, 11.
Pengelly, R. M. 1964, *M. N. R. A. S.*, **127**, 45.
Reynolds, R. J., Roesler, F., and Scherb, F. 1974, *Ap. J.* (Letters), **192**, L53.
Reynolds, R. J., Roesler, F., and Scherb, F. 1977, *Ap. J.*, **211**, 115.
Reynolds, R. J. 1980, *Ap. J.*, **226**, 153.
Reynolds, R. J. 1984, *Ap. J.*, **282**, 191.
Reynolds, R. J. 1987, *Ap. J.*, **323**, 553.
Scherb, F. 1981, *Ap. J.*, **243**, 644.
Stark, A. A., Bally, J., Linke, R. A., and Heiles, C. 1989, in preparation.
Van Woerden, H., Schwarz, U. J., and Hulsbosch, A. N. M. 1985, in *IAU Symposium 106, The Milky Way Galaxy*, eds R. J. Allen et al. (Dordrecht, Reidel), 387.